ECCOMAS Congress 2016
VII European Congress on Computational Methods in Applied Sciences and Engineering
M. Papadrakakis, V. Papadopoulos, G. Stefanou, V. Plevris (eds.)
Crete Island, Greece, 5–10 June 2016

A PATH-CONSERVATIVE OSHER-TYPE SCHEME FOR AXIALLY SYMMETRIC COMPRESSIBLE FLOWS IN FLEXIBLE TUBES

Julia Leibinger[1], Michael Dumbser[2] and Uwe Iben[1]

[1]Robert Bosch GmbH
Robert-Bosch-Campus 1, 71272 Renningen, Germany
e-mail: julia.leibinger@de.bosch.com

[2] Department of Civil, Environmental and Mechanical Engineering
University of Trento, Via Mesiano 77, 38123 Trento, Italy
e-mail: michael.dumbser@unitn.it

Keywords: compressible flows in compliant tubes, flexible ducts with variable cross section, fluid-structure interaction (FSI), visco-elastic wall behavior, non-conservative hyperbolic systems, path-conservative finite volume schemes.

Abstract. *In industrial applications there exist numerous hydraulic devices, as for example the fuel injection system in modern combustion engines, or hydraulic braking systems. These devices become more and more complex, and also the requirements concerning their efficiency are continuously increasing. Therefore, it is necessary to understand these systems well in order to optimize them already at the design stage. For that purpose, it is important to have a numerical simulation tool available that is able to calculate a solution for a given configuration quickly and accurately. In hydraulic devices, the different components, like pumps, valves or vessels, are usually connected via flexible tubes. Thus, the relevant physical effects of such compliant tubes must be considered in the numerical simulation, especially at high frequencies. In typical industrial applications, pressures can reach several thousand bar, hence the flow has to be usually considered as compressible, and at the same time also the visco-elastic behavior of the tube wall needs to be properly accounted for. Then, a suitable numerical method needs to be developed in order to solve the resulting partial differential equations (PDE) of this coupled fluid-structure interaction (FSI) problem accurately and efficiently.*
In our talk, the equations of an axially symmetric flow of a compressible barotropic fluid are considered for flows through flexible elastic and visco-elastic tubes, so that the dominant physical effects can be reproduced according to the composition of the tube wall. To calculate the numerical solution of the derived PDE, a path-conservative Osher-type solver - the so-called Dumbser-Osher-Toro (DOT)- is applied. This solver can deal with hyperbolic conservation laws that may also contain non-conservative products. To validate the proposed mathematical model and the numerical scheme, the numerical solutions are compared with analytical results derived in the frequency domain, as well as with experimental measurements. In both cases, the proposed path-conservative finite volume scheme based on the DOT Riemann solver produces very good results.

1 Introduction

Many industrial applications involve complex hydraulic systems. Their behavior needs to be understood already while designing and constructing the different components. Therefore, we need accurate mathematical models for the simulation of the dynamic behavior of the individual components of such hydraulic systems, which can be, for example, the fuel injection system into the combustion engine or the braking system in a car. Very often, flexible tubes are an important part of these complex systems, in order to connect the different components with each other. Hence, they have a very important influence on the overall behavior of the entire system. That is why in this paper we introduce a new mathematical model and provide a novel numerical solver in order to simulate the dynamic behavior of flexible tubes. The mathematical model represents the combined effects of the flow of a compressible barotropic fluid inside a flexible tube of circular cross section. Thus, the model accounts for the fluid-structure interaction (FSI) problem between a compressible fluid and the elastic behavior of the surrounding structure of the tube wall.
For the fluid we use the one-dimensional cross-sectionally averaged compressible Euler equations in a duct with variable circular cross section. For the material of the tube wall there exist various models [14]. For example, the Hooke's law can be applied to reproduce the elastic behavior of the tube in a rather simple way (see [11]). Another model is the so called Maxwell model. This model is built form springs and dash pots and can therefore reproduce the visco-elastic behavior of polymer material ([13]). Finally, we derive a system of non-conservative hyperbolic partial differential equations.
For solving the non conservative PDE system we apply the successful family of path-conservative schemes developed by Castro & Parés and co-workers [3, 20, 1, 12, 2, 18, 4, 5, 6], which are based on the theory of Dal Maso, Le Floch and Murat [17] on weak solutions for hyperbolic PDE with non-conservative products. In particular, we use an extension of the Riemann solver of Osher and Solomon [19] that was recently proposed by Dumbser and Toro in order to solve *general* conservative and non-conservative hyperbolic PDE systems [10, 9] (DOT). We combine these two solvers and apply them to our PDE system that describes the coupled fluid-structure interaction problem.
To verify the solver, some one-dimensional Riemann problems are solved, and the numerical solution is compared with a quasi-exact solution provided in [7], where also the fluid-structure-interaction is taken into account. To show that we are able to reproduce the visco-elastic behavior of real tubes with the Maxwell model, we compare it to an analytical solution derived in the frequency domain and to available experimental data [16].

2 The governing PDE system of the coupled FSI problem

To simulate the dynamic behavior of compressible fluids in flexible tubes we need to model the unsteady flow of a barotopic fluid through a tube with variable cross sectional area, as well as the elasticity of the tube wall. This results in a system of PDEs with a conservative and a non-conservative part.

2.1 The cross-sectionally averaged Euler equations for the fluid

The axially symmetric flow through a tube with variable cross-sectional area is described by the one dimensional cross sectionally averaged compressible Euler equations

$$\frac{\partial}{\partial t}(A\rho) + \frac{\partial}{\partial x}(A\rho u) = 0, \tag{1}$$

$$\frac{\partial}{\partial t}(A\rho u) + \frac{\partial}{\partial x}(A\rho u^2 + Ap) - p\frac{\partial A}{\partial x} = F_R. \tag{2}$$

In these equations $A(x,t)$ represents the variable cross sectional area, ρ the cross sectionally averaged density inside the tube, p the cross sectionally averaged pressure, u is the average velocity of the fluid and the term F_R accounts for the friction between fluid and wall (see for example [21]).
To characterize the dependency between pressure and density we assume a barotropic fluid. In this model, the pressure $p(\rho)$ only depends on the density. This so-called equation of state (EOS) also considers a two phase flow caused by cavitation, which appears, when the pressure drops below the vapor pressure p_v:

$$\rho(p) = \begin{cases} \rho_0 + \frac{1}{c_0^2}(p - p_v), & \text{if } p \geq p_v, \\ \frac{1}{\frac{\mu(p)}{\rho_v(p)} + \frac{1-\mu(p)}{\rho_0}}, & \text{if } 0 < p < p_v, \end{cases}, \tag{3}$$

where ρ_0 is the density at standard conditions and μ is the mass fraction of vapor $\mu(p) = -K(p - p_v)$, with a cavitaion constant K, the speed of sound c_0 of the fluid and the vapor density $\rho_v(p)$ calculated by the ideal gas law.

So far we only described the fluid, i.e. we still need an equation for the cross sectional area $A(x,t)$. In the next chapter we describe two models for the tube wall.

2.2 Material model for the visco-elastic tube wall

In this chapter we briefly describe two material models: first, a rather simple one, namely the Laplace law, where the cross sectional area only depends on the pressure and second, a more intricate one, the Maxwell model, where the time dependent visco-elastic behavior of the tube material is also taken into account.

2.2.1 The Laplace law

With the Laplace law, a linear Hooke-like behavior is described. In the so derived model the cross sectional area is only affected by the current local pressure inside the tube,

$$A = A_0 + \frac{1}{\beta}(p - p_{ext}), \tag{4}$$

with the equilibrium cross sectional area A_0, the elasticity constant β and the external pressure p_{ext}.

2.2.2 The Maxwell model

The previously described Laplace law has only a limited validity for real materials. For polymer tubes we also need to consider the time dependent behavior of the material. Therefore a Maxwell model composed of springs and dash pots is applied. In Figure 1 a schematic representation of such a model is shown.

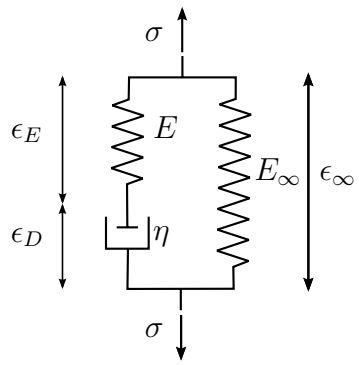

Figure 1: Schematic representation of a 3-parameter Maxwell model.

From this combination of springs and dash pots the following PDE results

$$\frac{\partial \phi}{\partial t} = -\frac{1}{\frac{E_0 \phi}{2Wc^2} + \rho} \frac{\partial (\phi \rho u)}{\partial x} + \frac{(2W(p - p_{ext}) - (\phi - 1)E_\infty)\,\phi}{\tau_1 (2Wc^2\rho + E_0\phi)}, \tag{5}$$

with $\phi = \frac{A}{A_0}$ the normalized cross sectional area, the elasticity constants E_∞ and $E_0 = E_\infty + E$, the relaxation parameter $\tau_1 = \frac{E}{\eta}$, the fluid density ρ, the fluid velocity u, the fluid pressure p and the speed of sound c of the fluid. W is a geometry factor that represents the wall thickness and is defined as follows:

$$W = 2\frac{\left(\frac{r_a}{r_i}\right)(1+\nu) + 1 - 2\nu}{\left(\frac{r_a}{r_i}\right)^2 - 1}, \tag{6}$$

with the inner and outer radius r_i and r_a and the Poisson ratio ν. For a more detailed description of the material models, see [13, 15]

3 The DOT Riemann solver

The equations described in the previous chapter need to be solved. We derive a system of PDEs with a conservative and non-conservative part. Such equations read as follows:

$$\frac{\partial \mathbf{Q}}{\partial t} + \frac{\partial}{\partial x}\mathbf{f}(\mathbf{Q}) + \mathbf{B}(\mathbf{Q})\frac{\partial \mathbf{Q}}{\partial x} = \mathbf{S}(\mathbf{Q}). \tag{7}$$

Here, $\mathbf{Q}(x,t) \in \mathrm{R}^n$ is the state vector, $\mathbf{f}(\mathbf{Q})$ is a nonlinear flux that contains the conservative part and $\mathbf{B}(\mathbf{Q})$ is an $n \times n$ matrix that includes the purely non-conservative part of the system. $\mathbf{S}(\mathbf{Q})$ is a nonlinear algebraic source term which results from the friction model F_R and the Maxwell model.

To solve the equations we unify two solvers in order to get a new solver that can handle both, a conservative an non-conservative part. The basic ideas of both solvers is the Riemann solver of Osher an Solomon and its extension to *general* hyperbolic systems described in [10, 9]. To get the combined solver the equation (7) needs to be reformulated as follows

$$\frac{\partial \mathbf{Q}}{\partial t} + \mathbf{A}(\mathbf{Q})\frac{\partial \mathbf{Q}}{\partial x} = \mathbf{S}(\mathbf{Q}), \tag{8}$$

with the new system matrix $\mathbf{A}(\mathbf{Q}) = \partial \mathbf{f}/\partial \mathbf{Q} + \mathbf{B}(\mathbf{Q})$. Now the finite volume scheme is written like

$$\mathbf{Q}_i^{n+1} = \mathbf{Q}_i^n - \frac{\Delta t}{\Delta x}\left(\mathbf{f}_{i+\frac{1}{2}} - \mathbf{f}_{i-\frac{1}{2}}\right) - \frac{\Delta t}{\Delta x}\left(\mathbf{D}_{i+\frac{1}{2}} + \mathbf{D}_{i-\frac{1}{2}}\right) - \Delta t \mathbf{B}(\mathbf{Q}_i^{n+\frac{1}{2}})\frac{\Delta \mathbf{Q}_i^n}{\Delta x} + \Delta t \mathbf{S}(\mathbf{Q}_i^{n+\frac{1}{2}}). \tag{9}$$

In this equation the numerical flux is defined by

$$\mathbf{f}_{i+\frac{1}{2}} = \frac{1}{2}\left(\mathbf{f}(\mathbf{Q}^+_{i+\frac{1}{2}}) + \mathbf{f}(\mathbf{Q}^-_{i+\frac{1}{2}})\right) - \frac{1}{2}\int_0^1 \left|\mathbf{A}\left(\Psi(\mathbf{Q}^-_{i+\frac{1}{2}}, \mathbf{Q}^+_{i+\frac{1}{2}}, s)\right)\right| \frac{\partial \Psi}{\partial s} ds \tag{10}$$

and the so called jump terms by

$$\mathbf{D}_{i+\frac{1}{2}} = \frac{1}{2}\int_0^1 \mathbf{B}\left(\Psi(\mathbf{Q}^-_{i+\frac{1}{2}}, \mathbf{Q}^+_{i+\frac{1}{2}}, s)\right) \frac{\partial \Psi}{\partial s} ds. \tag{11}$$

The path Ψ is connecting the left state $\mathbf{Q}^-_{i+\frac{1}{2}}$ with the right state $\mathbf{Q}^+_{i+\frac{1}{2}}$. In our calculation we use a simple linear path and the path integrals are computed *numerically* via a simple Gauss-Legendre quadrature rule, so we get the final formulations

$$\mathbf{f}_{i+\frac{1}{2}} = \frac{1}{2}\left(\mathbf{f}(\mathbf{Q}^+_{i+\frac{1}{2}}) + \mathbf{f}(\mathbf{Q}^-_{i+\frac{1}{2}})\right) - \frac{1}{2}\left(\sum_{j=1}^{N_G} \omega_j \left|\mathbf{A}\left(\Psi(\mathbf{Q}^-_{i+\frac{1}{2}}, \mathbf{Q}^+_{i+\frac{1}{2}}, s_j)\right)\right|\right)\left(\mathbf{Q}^+_{i+\frac{1}{2}} - \mathbf{Q}^-_{i+\frac{1}{2}}\right) \tag{12}$$

and

$$\mathbf{D}_{i+\frac{1}{2}} = \frac{1}{2}\left(\sum_{j=1}^{N_G} \omega_j \mathbf{B}\left(\Psi(\mathbf{Q}^-_{i+\frac{1}{2}}, \mathbf{Q}^+_{i+\frac{1}{2}}, s_j)\right)\right)\left(\mathbf{Q}^+_{i+\frac{1}{2}} - \mathbf{Q}^-_{i+\frac{1}{2}}\right). \tag{13}$$

For a more detailed description of the solver see [15].

4 Numerical results

We verify the solver by comparing it to a quasi-exact solution ([7, 8]) by solving the Riemann problems defined in Table 1. An exact solution can only be obtained for the Laplace law, since the Maxwell model is time dependent, which introduces a source term on the right hand side of the PDE system. To validate the physical behavior of the Maxwell model, we compare it to analytical and experimental results in the frequency domain.

4.1 Riemann problems

We present the solution of two Riemann problems. The Riemann problem one remains in the fluid domain whereas the second Riemann problem results in two phase flow. The results for the calculations with the Laplace law and the comparison with the quasi-exact solution are shown in Figs. 2 and 3 for the time $t_{end} = 4 \cdot 10^{-4}$. The agreement between both solutions is good.

Additionally, Figs. 4 and 5 illustrate the solutions of the Maxwell model for the time $t_{end} = 8 \cdot 10^{-4}$ for the same initial condition. The parameters for the Maxwell model are $E_0 = 10^9$ and $E_\infty = 0.9 \cdot 10^9$ ant $\eta = 2 \cdot 10^4$. The time dependency of the model can be clearly seen, when

we compare the results to the one obtained with the Laplace law, where the wave profiles are sharper.

case	p_L	u_L	p_R	u_R	β	number of cells
RP1	$8 \cdot 10^5$	0	$2 \cdot 10^5$	0	$4.38 \cdot 10^{13}$	200
RP2	$2 \cdot 10^4$	0	$2 \cdot 10^2$	0	$4.38 \cdot 10^{13}$	500

Table 1: Initial states for Riemann problems (p[Pa], u[m/s])

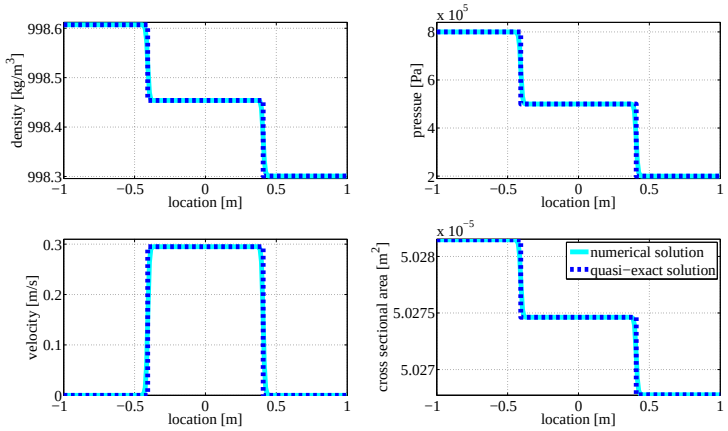

Figure 2: Riemann problem for the Maxwell model with in liquid domain and comparison to quasi-exact solution.

4.2 Comparison with experimental results

To show that the Maxwell model can actually reproduce the behavior of real tube materials, the numerical results are compared to experimental ones and to analytical solutions obtained in the frequency domain. In the experimental setup, the test object was excited with frequencies between 0 and 2000 Hz, then volumetric flow rate and the pressure were measured at the in- and outlet. The exact method is described in [16]. In Fig. 6 one can see the results. The green dotted lines are the experimental results, the dashed lines are the analytical reference solution obtained in the frequency domain and the solid lines are the solutions obtained from the numerical simulations obtained with the previously described numerical method and mathematical model. The calculations are done with and without friction model. For frequencies up to 800 Hz one can see a good agreement. Beyond 800 Hz, the agreement with experiments is worse. This could have two possible reasons: first, the quality of the experimental results seems to deteriorate, which is visible from the unphysical jumps in the experimental results beyond 800 Hz. Second, a higher order Maxwell model, which means a Maxwell model with more springs and dash pots in parallel could improve the accuracy of the numerical simulation.

5 Conclusion

We presented a nonconservative system of nonlinear hyperbolic PDEs in one space dimension for the simulation of compressible fluid flow in flexible tubes. We showed that we can reproduce experimental results with the Maxwell model. The numerical solver introduced for solving the governing PDE system (DOT) was also validated with a quasi-exact solution.

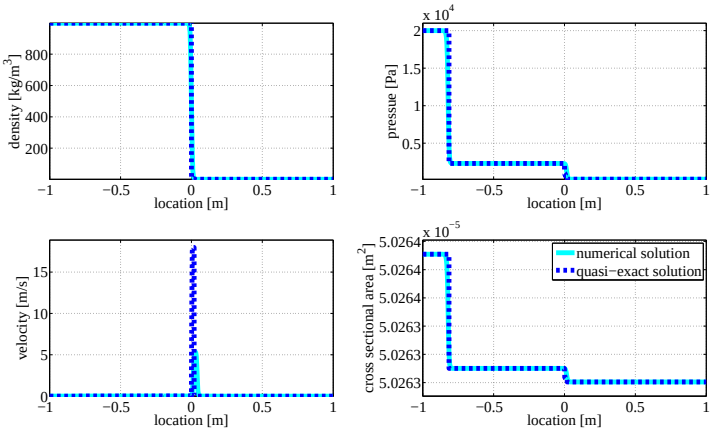

Figure 3: Riemann problem for the Laplace law with two phase flow and comparison to quasi-exact solution.

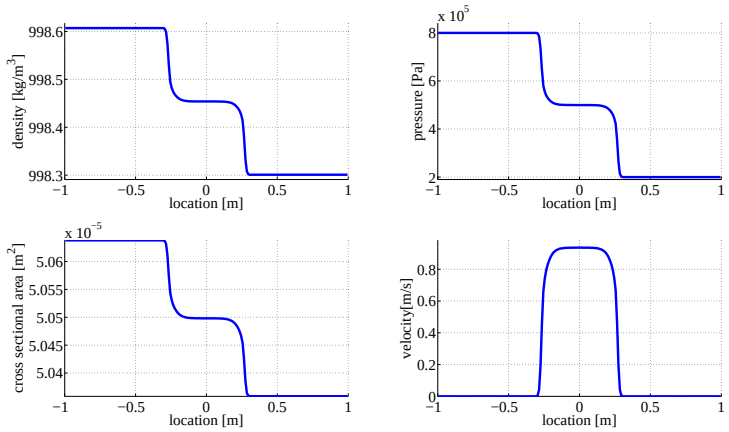

Figure 4: Riemann problem for the Maxwell model with in liquid domain.

Future work will also consider the modelling of more complex tubes, like multi-layered hydraulic tubes. These tubes have shown a different dynamic behavior in experiments and this behavior could not be well reproduced with the equations explained in this paper. Therefore the equations need to be modified and the numerical solver needs to be adapted to solve these new equations.

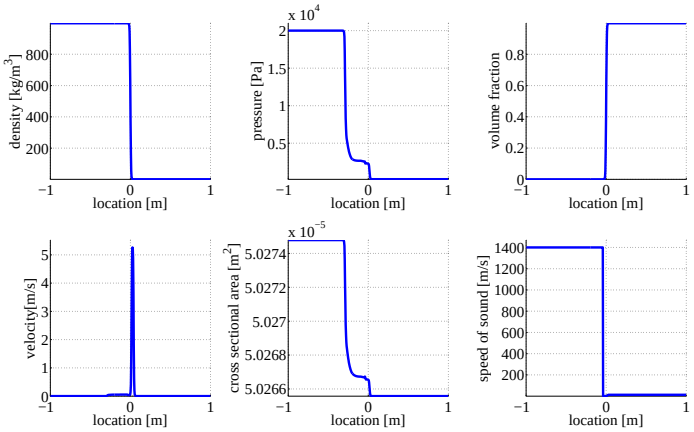

Figure 5: Riemann problem for the Maxwell model with two phase flow.

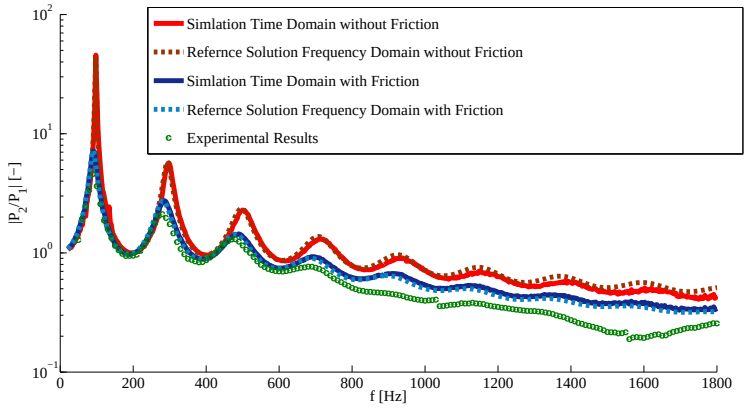

Figure 6: Comparison with experimental results in the frequency domain.

REFERENCES

[1] M. CASTRO, E. FERNÁNDEZ, A. FERRIERO, J. GARCÍA, AND C. PARÉS, *High order extensions of Roe schemes for two dimensional nonconservative hyperbolic systems*, Journal of Scientific Computing, 39 (2009), pp. 67–114.

[2] M. CASTRO, J. GALLARDO, J. LÓPEZ, AND C. PARÉS, *Well-balanced high order extensions of Godunov's method for semilinear balance laws*, SIAM Journal of Numerical Analysis, 46 (2008), pp. 1012–1039.

[3] M. CASTRO, J. GALLARDO, AND C. PARÉS, *High-order finite volume schemes based on reconstruction of states for solving hyperbolic systems with nonconservative products. applications to shallow-water systems*, Mathematics of Computation, 75 (2006), pp. 1103–1134.

[4] M. CASTRO, A. PARDO, C. PARÉS, AND E. TORO, *On some fast well-balanced first order solvers for nonconservative systems*, Mathematics of Computation, 79 (2010), pp. 1427–1472.

[5] M. DUMBSER, M. CASTRO, C. PARÉS, AND E. TORO, *Ader schemes on unstructured meshes for nonconservative hyperbolic systems: Applications to geophysical flows*, Computers & Fluids, 38 (2009), pp. 1731 – 1748.

[6] M. DUMBSER, A. HIDALGO, M. CASTRO, C. PARÉS, AND E. TORO, *Force schemes on unstructured meshes ii: Non-conservative hyperbolic systems*, Computer Methods in Applied Mechanics and Engineering, 199 (2010), pp. 625 – 647.

[7] M. DUMBSER, U. IBEN, AND M. IORIATTI, *An efficient semi-implicit finite volume method for axially symmetric compressible flows in compliant tubes*, Applied Numerical Mathematics, 89 (2015), pp. 24–44.

[8] M. DUMBSER, U. IBEN, AND C. MUNZ, *Efficient implementation of high order unstructured WENO schemes for cavitating flows*, Computers & Fluids, 86 (2013), pp. 141 – 168.

[9] M. DUMBSER AND E. F. TORO, *On universal Osher–type schemes for general nonlinear hyperbolic conservation laws*, Communications in Computational Physics, 10 (2011), pp. 635–671.

[10] ——, *A simple extension of the Osher Riemann solver to non-conservative hyperbolic systems*, Journal of Scientific Computing, 48 (2011), pp. 70–88.

[11] R. ETLENDER, *Modellierung und Simulation der Wellenausbreitung in flexiblen hydraulischen Leitungen*, PhD thesis, Universität Stuttgart, 2012.

[12] J. GALLARDO, C. PARÉS, AND M. CASTRO, *On a well-balanced high-order finite volume scheme for shallow water equations with topography and dry areas*, Journal of Computational Physics, 227 (2007), pp. 574–601.

[13] M. GOEKE, *Modellierung der Materialdmpfung bei der Wellenausbreitung in flexiblen Leitungen*, master's thesis, University Stuttgart, 2013.

[14] R. LAKES, *Viscoelastic Solids*, CRC Press Inc, 1998.

[15] J. LEIBINGER, M. DUMBSER, U. IBEN, AND I. WAYAND, *A path-conservative osher-type scheme for axially symmetric compressible flows in flexible visco-elastic tubes*, Applied Numerical Mathematics, (2016).

[16] R. LEONHARDT, *Dynamische Untersuchungen von Hydraulikkomponenten*, PhD thesis, Universitt Karlsruhe, 2008.

[17] G. D. MASO, P. LEFLOCH, AND F. MURAT, *Definition and weak stability of nonconservative products*, J. Math. Pures Appl., 74 (1995), pp. 483–548.

[18] M. MUÑOZ AND C. PARÉS, *Godunov method for nonconservative hyperbolic systems*, Mathematical Modelling and Numerical Analysis, 41 (2007), pp. 169–185.

[19] S. OSHER AND F. SOLOMON, *Upwind difference schemes for hyperbolic systems of conservation laws*, Math. Comp., 38 (1982), pp. 339–374.

[20] C. PARS, *Numerical methods for nonconservative hyperbolic systems: a theoretical framework.*, SIAM Journal on Numerical Analysis, 44 (2006), pp. 300–321.

[21] W. ZIELKE, *Frequency-dependent friction in transient pipe flow*, Journal of Basic Engineering, 90 (1968), pp. 109–115.